Thermoplastic Corn Starch Reinforced with Cotton Cellulose Nanofibers

Eliangela de M. Teixeira,[1] Cybele Lotti,[1] Ana C. Corrêa,[1] Kelcilene B. R. Teodoro,[1,2] José M. Marconcini,[1] Luiz H. C. Mattoso[1]

[1]*National Nanotechnology Laboratory for Agriculture (LNNA), Embrapa Agricultural Instrumentation, 13560-970 São Carlos, SP, Brazil*
[2]*Federal University of São Carlos (UFSCar), Chemical Department, 13565-905 São Carlos, SP, Brazil*

Received 13 June 2010; accepted 26 September 2010
DOI 10.1002/app.33447
Published online 10 December 2010 in Wiley Online Library (wileyonlinelibrary.com).

ABSTRACT: This work evaluates the use of cotton cellulose nanofibers (CCN) as a reinforcing agent to prepare thermoplastic corn starch (TPS) matrix plasticized with 30 wt % of glycerol. The nanocomposites were filled with 0.5–5.0 wt % of CCN on a dry-starch basis. The dried nanofibers were resuspended through the use of an ultrasonicator and then introduced in the fixed water formulation for obtaining TPS. The nanocomposites were compounded in a corotating twin-screw extruder. Scanning transmission electron microscopy (STEM), field emission gun (FEG), X-ray diffraction (XRD) and thermogravimetric analysis (TGA), in air atmosphere, were used to characterize nanofibers, neat TPS, and nanocomposites. The results showed that the nanofibers had needlelike structure with an average length of about 135 ± 50 nm and an average diameter of about 14 ± 4 nm. The addition of CCN was effective to enhance the mechanical properties of neat TPS in compositions above 2.5 wt %, although some agglomeration could be observed. The resulting nanocomposites showed good structural stability, because the amylopectin transcrystallization phenomena on the surface of nanofibers had not occurred. Only a slight decrease in the crystallinity index and a minor increase in the water absorption in relation to neat TPS were observed. An increase in the thermal stability of TPS nanocomposites with respect to neat TPS was verified, but it was independent of the CCN content. © 2010 Wiley Periodicals, Inc. J Appl Polym Sci 120: 2428–2433, 2011

Key words: plasticized starch; cellulosic nanocomposites; cotton nanofibers

INTRODUCTION

Because of their low cost, wide abundance, renewable, and environmental-friendly characteristic, and outstanding capacity to reinforce polymeric matrices, the utilization of cellulose in nanoscale to obtain cellulosic nanocomposites has been a great deal of study in this area.[1–4] Nanocellulose can be obtained by acid hydrolysis treatment of cellulose under controlled time and temperature conditions. This process results in disruption of amorphous regions into cellulose structure, while the crystalline regions remain intact.[1,5] After hydrolysis, a suspension of needlelike particles with length of the order of few hundred nanometers and diameter of few nanometers can be obtained.

The main difficulty in producing polymeric nanocomposites filled with cellulose nanofibers is the poor dispersion and compatibility with nonpolar solvents and nonpolar matrices due to the strong hydrogen bonds between adjacent cellulose fibers.[5,6] It causes nanofibers' agglomeration and, consequently, endangers the effectiveness of mechanical reinforcement. Several strategies used to overcome this undesirable effect are reported in the work of Hubbe et al.,[1] Eichhorn et al.,[3] and Dufresne and Belgacem.[2] Dispersion of nanofibers in an organic solvent, chemical modification, or grafting on nanofibers surface have being tested. In the case of hydrosoluble matrices, like starch, the nanocomposites are obtained by casting method. The majority of works regarding the obtaining of nanocomposites based on starch and cellulose nanofibers reported good dispersion and, overall, good performance using this method.[7–16] However, only few works have studied the incorporation of nanocellulose on starch-based materials using conventional methods of polymer processing in the melt state. Teixeira et al.[17] had incorporated cassava bagasse nanofibers in the thermoplastic cassava starch using a torque rheometer. The nanofibers seemed to be fairly dispersed in the thermoplastic corn starch (TPS) matrix, but their reinforcement effect was limited due to the presence of other components in the nanofibers suspension, like sugars.

In this work, we propose the incorporation of cotton nanofibers in the water matrix composition. The TPS nanocomposites were processed in a corotating

Correspondence to: L. H. C. Mattoso (mattoso@cnpdia.embrapa.br).

twin-screw extruder and characterized by means of index of crystallinity, moisture-absorption content, thermogravimetric behavior on air atmosphere, tensile properties, and image analysis.

EXPERIMENTAL

Preparation of cotton nanofibers

Cotton cellulose nanofibers (CCN) were obtained by acid hydrolysis of white cotton (commercial type) as describe elsewhere.[18] Briefly, the cotton fibers were finely chopped in a knife mill (Solab) passed through a 10-mesh sieve, dried at 50°C, and hydrolyzed in 6.5*M* sulfuric acid (Synth) solution at 45°C for 75 min. Then, the sulfuric acid was partially removed from the resulting suspension by successive centrifugations (Sorvall® Super T21) at 10,000 rpm for 10 min. Following, the resulting suspension was submitted to dialysis in a cellulose membrane (Sigma-Aldrich-D9402) until pH 6–7 was reached. The resulting suspension was ultrasonicated for 5 min through the use of a Branson 450 sonicator and dried at 35°C for 12 h in an air-circulating oven.

Preparation of nanocomposites reinforced with cellulose cotton nanofibers

Corn starch containing about 24% amylose was kindly supplied by Corn Products, Brazil. Reagent grade glycerol (Synth, 30 wt %, based on dry starch) was used as a plasticizer. Stearic acid and citric acid (both from Synth and 2 wt %, based on dry starch) were used as antioxidant agents. For the preparation of nanocomposites, the dry CCN was first redispersed in the water of the composition (the final water content for all samples was fixed in 20 wt %-dry starch basis) using a sonificator (Branson 450) for 5 min, and it was composed of finely dispersed nanofibers in distinct concentrations 0.5, 1.5, 2.5, 3.5, and 5 wt % (dry starch basis). The resulting suspension was added to the system starch + glycerol + stearic acid + citric acid. The resulting mixture was manually homogenized, and the nanocomposites were processed in a twin-screw extruder (Coperion) through the use of a temperature profile between 140 and 160°C. The films were obtained by hot-pressing process at 160°C, under a force of 10 metric tons and for 5min after a prefusion of 5 min.

Nanocomposite conditioning and water uptake

The nanocomposites were dried at 70°C until a constant weight was reached. They were further conditioned before each analysis in hermetic containers at 25°C ± 2°C and in a 53% RH atmosphere in equilibrium with a saturated solution of Mg $(NO_3)_2 \cdot 6H_2O$, as defined in ASTM E104. Water-uptake experiments were conducted in circular specimens, cut from the prepared hot-pressed plaques, with diameter of 8 and 2-mm thick. The water uptake after 30 days was computed from the gain in weight.

Scanning transmission electron microscopy

Scanning transmission electron microscopy (STEM) analysis was performed in a Tecnai™ G2 F20 equipment. The images were acquired with a bright-field detector. A droplet of diluted nanofiber suspension was deposited on a carbon microgrid (400 mesh) and allowed to dry. The grid was stained with a 1.5% solution of uranyl acetate and dried at room temperature.

Field emission gun scanning electron microscopy

The morphology of the granular corn starch and the cryogenic-fractured surface of both neat TPS and nanocomposites were investigated by field emission gun scanning electron microscopy (FEG–SEM) using a PHILLIPS-XL30 FEG-SEM instrument. The samples were sputtered with a thin layer of gold (~ 15 nm).

X-ray diffraction

The X-ray diffraction (XRD) patterns for CCN were obtained with an X-ray diffractometer (VEB Carl Zeiss-Jena URD-6 Universal Diffractometer) using Cu Kα radiation (λ = 1.5406 A) at 40 kV and 20 mA. Scattered radiation was detected in the range of 2θ = 5°–40° at a scan rate of 2°/min. The crystallinity index (C_I) for CCN was calculated through the height of the 200 peak (I_{200}, 2θ = 22.6°) and the minimum intensity between the 200 and 110 peaks (I_{am}, 2θ = 18°), using the Buschle–Diller–Zeronian equation [eq. (1)].[19] I_{200} represents both crystalline and amorphous components, while I_{am} represents the amorphous component.

$$C_I(\%) = \left(1 - \frac{I_{am}}{I_{200}}\right) \times 100 \quad (1)$$

The diffractograms for nanocomposites were recorded after the conditioning of the samples. Their crystallinity index was estimated by the height ratio of the diffraction peak (B-type at 2θ = 16.8° and V_H-type at 2θ = 19.6°) and the baseline of the diffractogram, as proposed by Hulleman et al.[20]

Thermogravimetric analysis

The CCN and nanocomposites were subjected to thermogravimetric analysis (TGA) in a TA Q500 thermal analyzer (TA Instruments, New Castle, DE).

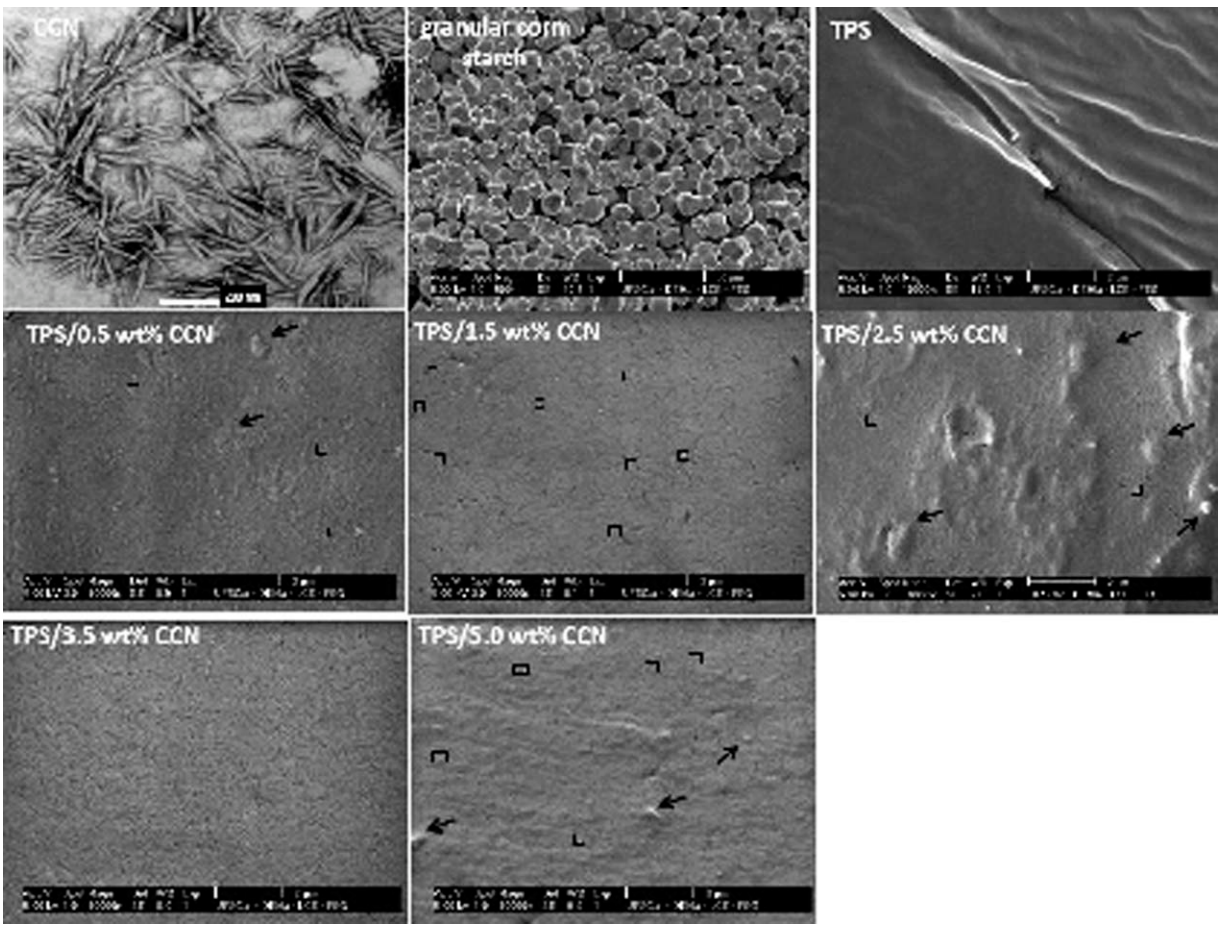

Figure 1 Micrograph of STEM for CCN and micrograph of FESEM for granular corn starch, thermoplastic corn starch (TPS), and its nanocomposites.

The samples (10 ± 1 mg) were heated in a Pt crucible from 25 to 600°C in air flowing at 60 mL min^{-1}. The heating rate was 10°C min^{-1}. The initial temperatures of the thermal degradation (T_{id}) were obtained from the onset points of the TGA curves.

Tensile tests

The tensile properties were measured in accordance with ASTM D638-96 type II requirements. An Instron 5500R Universal Test Instrument equipped with a load cell of 500 kgf, and a crosshead speed of 50 mm/min was used. The previously conditioned samples were tested. The tensile modulus was calculated through the slope of the initial and linear part of the stress–strain curve. The mechanical tensile data were automatically calculated by the software, and at least five specimens were tested.

RESULTS AND DISCUSSION

Morphology

STEM observations (Fig. 1) showed the individual nanofibers obtained after the acid extraction. Needle-like structure was observed, with an average dimension of about 14 ± 4 nm in diameter and 135 ± 50 nm in length as determined in our previous study.[18] Figure 1 also shows FEG–SEM images of granular corn starch, plasticized corn starch (TPS), and cryogenic-fractured surfaces of both TPS and its nanocomposites. The starch granule size was around 8–15 μm, and their complete disruption could be observed through TPS and nanocomposites micrographs. The neat TPS and its nanocomposites showed high sensitivity to the electron beam. Thus, some surface cracks could be observed. The CCN are shown in the STEM images as shinny spots, with diameters in the range of 60–330 nm, representing the nanofibers' cross section, as also reported in literature.[5,7] The observed diameters are an evidence of some degree of agglomeration, especially for 2.5 wt % and above CCN content nanocomposites. In Figure 1, individual spots are contoured by squares, while agglomerates are signalized by arrows. However, it is worth noting that, in the nanocomposites with 3.5 and 5.0 wt % CCN, this visualization became more difficult, as an indicative of better wettability of CCN within the matrix.

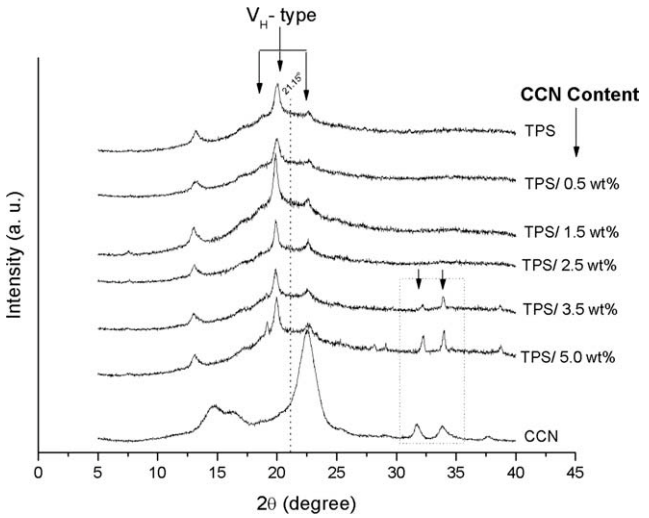

Figure 2 X-ray diffraction patterns of TPS, CCN, and nanocomposites.

XRD and water absorption

The X-ray diffraction (XRD) patterns recorded for CCN and TPS nanocomposites after conditioning are shown in Figure 2. The CCN diffractrogram displayed well-defined peaks, typical of a highly crystalline structure. The peak at $2\theta = 14.7°$, $2\theta = 16.3°$, $2\theta = 22.6°$, and $2\theta = 34.7°$ corresponds to the (101), (10-1), (002), and (040) crystallographic planes, respectively,[21,22] which are characteristic for cellulose type I.[23] The crystallinity index was calculated by eq. (1) and found to be 91% for CCN. This high crystallinity is characteristic for nanocellulose obtained by acid process. The nanocomposite samples did not show a peak around $2\theta = 16.8°$ characteristic of amylopectin recrystallization (B-type crystallization) indicating no residual crystallinity due to granules presence after the extrusion. The processing-induced crystallization can occur as a recrystallization of a single-helical structure of amylose during cooling after processing. It corresponds to V_H-type, and it is mainly characterized by the intense peak at $2\theta = 19.6°$. The V_H-type consists of amylose recrystallization induced by lysophospholipids and complex-forming agents such as isopropanol and glycerol. The diffraction peaks regarding to only CCN crystalline structures at $2\theta = 14.5°$ and $2\theta = 16.3°$ were not clearly observed in the nanocomposites' diffractograms. The CCN peak at $2\theta = 22.6°$ was overlapping the TPS diffraction pattern. Nevertheless, the nanocomposite with CCN content above 2.5 wt %, characteristic for CCN peaks at $2\theta = 32.5°$ and $2\theta = 34.7°$, could be observed.

The crystallinity index of the nanocomposites was estimated from the magnitude of the diffraction peak at $2\theta = 19.6°$, as reported in the Experimental section. These results are shown in Table I as well as the results of water uptake after conditioning. It could be observed that the incorporation of CCN to TPS matrix did not alter significantly the V_H-type crystallinity of the nanocomposites, except for the nanocomposite with 1.5 wt % CCN. In this case, the higher water uptake could have favored the molecular arrangements of TPS chain, inducing a higher crystallinity index for this sample. On the other hand, a small decrease of crystallinity could be observed in some samples. This feature was also observed by Mathew et al.[9] in thermoplastic starch plasticized with sorbitol and reinforced with tunicin whiskers at high-filler loads (15 wt % with respect to starch/glycerol weight). The crystallinity reduction was attributed to the decrease in the rearrangement resistance of the starch chains due to the transcrystallization of amylopectin in the nanofiber surface. This is a consequence of the coating of cellulose nanofibers by glycerol plasticizer, as firstly reported by Angles and Dufresne,[7] being characterized by the presence of a peak at $2\theta = 21.15°$.[7,8] This phenomenon hinders the stress transfer in the filler-matrix interface, compromising the reinforcement effect of the nanocellulose filler.

However, in the present work, this peak at $2\theta = 21.15°$ could not be observed. Possibly, the additional use of citric acid to prevent the retrogradation of amylose chains could also have inhibited the amylopectin transcrystallization phenomenon. Except for the sample with 1.5 wt % CCN, no significant difference in water uptake could be detected among the nanocomposites. But, with respect to neat TPS, a slight increase of water absorption could be verified.

Thermogravimetric analysis

The thermal behavior of CCN, TPS, and nanocomposites under air atmosphere is presented in Figure 3. By the TG curves [Fig. 3(a)], the initial temperatures of the thermal degradation (considering T_{id} the onset point) were determined, and they are shown in Table II. The data show that the neat TPS has a lower

TABLE I
Crystallinity Index (V_H-type) and Water Uptake after 30 days of Conditioning at 25°C ± 2°C and 53% RH) for Neat TPS and Nanocomposite Samples

Sample	V_H-type crystallinity index ($2\theta = 19.6°$)	Water uptake after 30 days (%)
TPS	45	5.32 ± 0.18
TPS/0.5 wt % CCN	44	6.17 ± 0.17
TPS/1.5 wt % CCN	50	7.18 ± 0.03
TPS/2.5 wt % CCN	47	6.50 ± 0.19
TPS/3.5 wt % CCN	45	6.10 ± 0.11
TPS/5.0 wt % CCN	43	6.10 ± 0.09

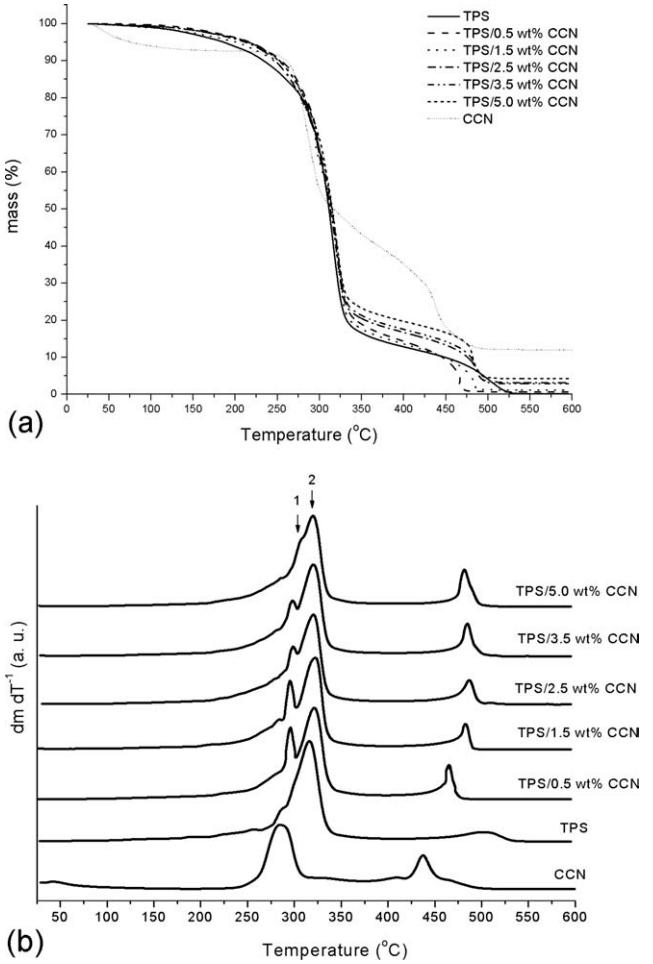

Figure 3 (a) TG and (b) DTG curves of TPS, CCN, and nanocomposites. Heating at 10°C min^{-1} in air atmosphere.

thermal stability than CCN and that nanocomposites have a better thermal stability than the TPS matrix. According to Table II data, there was an increase from 35 to 45°C (17.5–22.5%) in the T_{id} of the nanocomposites in comparison with neat TPS. The behavior of the resulting nanocomposites is quite interesting when they are blended with other polymers that require higher processing temperature. But, independently of the CCN content, the T_{id} of the nanocomposites is similar. On the DTG curves [Fig. 3(b)], in the temperature range from 250 to 350°C, two main thermal events [codified in the Fig. 3(b) as 1 and 2 peaks] are shown, and their maximum degradation (T_{max}) temperatures are shown in Table II. The peak 1 (next to 285°C) coincides with the degradation processes of both TPS and CCN. The peak 2 (between 300 and 350°C) was attributed to the thermal degradation of neat TPS and TPS matrix in the nanocomposites. We can observe that the peak 1 in nanocomposites containing 2.5 wt % of CCN and above has the slight tendency to shift to higher temperatures toward T_{Max2} (see Table II) suggesting changes on the thermal degradation mechanism of these TPS nanocomposites. The events that occur at temperatures greater than 500°C [Fig. 3(a)] correspond to the degradation of carbonaceous residues, which rise with the increase of CCN content.

TABLE II
Thermal Properties of CCN, TPS, and Respective Nanocomposites Obtained by TGA Analyses

Sample	T_{id} (°C)	$T_{Max\ 1}$ (°C)	$T_{Max\ 2}$ (°C)
TPS	200	285	315
CCN	260	285	***
TPS/0.5 wt % CCN	235	295	322
TPS/1.5 wt % CCN	237	295	322
TPS/2.5 wt % CCN	235	300	322
TPS/3.5 wt % CCN	245	300	322
TPS/5.0 wt % CCN	245	305	322

Tensile testing

The tensile properties of TPS and its nanocomposites are presented in Figure 4. It can be observed that, in general, the nanocomposites showed higher tensile properties than neat TPS. An unconventional increase of up to 122% in the elongation at break with the addition of CCN was achieved. Such behavior was also reported by Kvien et al.,[10] with the system comprised modified potato starch plasticized with D-sorbitol reinforced by cellulose whiskers obtained from microcrystalline cellulose and by Teixeira et al.,[17] with cassava starch plasticized with glycerol and reinforced with cassava

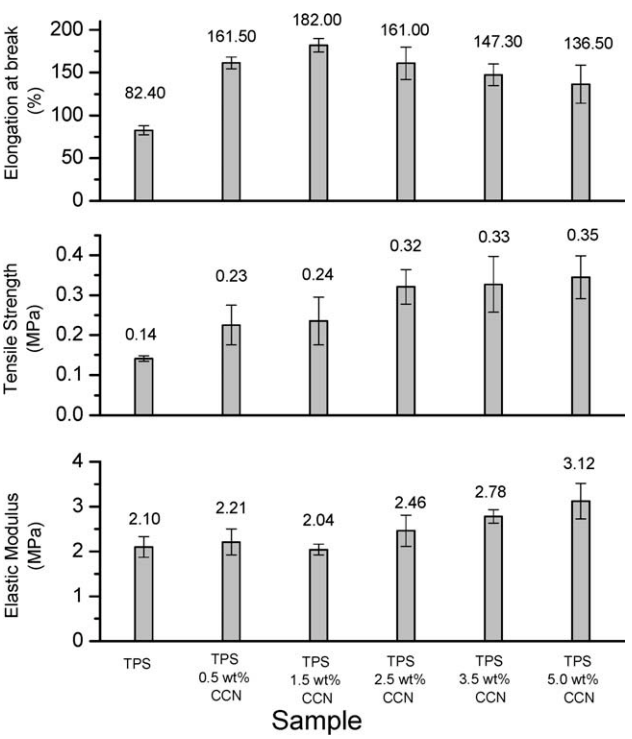

Figure 4 Tensile properties of TPS and nanocomposites.

bagasse cellulose nanofibrils. The processing conditions, the presence of sugars in the nanofibrils suspension, and the increase of water uptake in comparison to neat TPS were reported as possible causes for the increase in elongation at break. Furthermore, a slight increase of water uptake was also verified in this present work (see Table I). Thus, the higher moisture content on the sample could result in an additional plasticizer effect on the TPS chains. This behavior was more noticeable in the sample with 1.5 wt % CCN. Both elastic modulus and tensile strength results revealed that the reinforcement effect of CCN is more pronounced for composition above 2.5 wt % CCN content. In comparison with neat TPS, these properties were improved up to 48.5 and 150%, respectively, for the composition with 5 wt % CCN, indicating a synergistic effect of the nanofibers on the TPS matrix. An increase of 24.3[10] and 73%[11] in the elastic modulus had been reported for thermoplastic starches reinforced with 5 wt % nanofibers. However, different starch and nanofibers sources, further than distinct processing method, were used.

CONCLUSIONS

Nanocomposites based on corn thermoplastic starch and CCN were obtained by conventional extrusion process. Even though some extent of nanofibers agglomeration was attained, the presence of CCN in concentration above 2.5 wt % could improve the elastic modulus, tensile strength, and elongation at break of the TPS matrix. The incorporation of CCN slightly reduced the crystallinity and increased the hygroscopic behavior of the TPS matrix. That incorporation also increased the thermal stability of TPS nanocomposites with respect to neat TPS, but it was independent of the CCN content.

References

1. Hubbe, M. A.; Rojas, O. J.; Lucia, L. A.; Sain, M. Bioresources 2008, 3, 929.
2. Dufresne, A.; Belgacem, M. N. Polím Ciê Tecnolgia 2010, 20.
3. Eichhorn, S. J.; Dufresne, A.; Aranguren, M.; Marcovich, N. E.; Capadona, J. R.; Rowan, S. J.; Weder, C.; Thielemans, W.; Roman, M.; Renneckar, S.; Gindl, W.; Veigel, S.; Keckes, J.; Yaho, H.; Abe, K.; Nogi, M.; Nakagaito, A. N.; Mangalam, A.; Simonsen, J.; Benight, A. S.; Bismarck, A.; Berglund, L. A.; Peijs, T. J Mater Sci 2009, 45, 1.
4. Habibi, Y.; Lucia, L. L.; Rojas, O. J Chem Rev 2010, 110, 3479.
5. Dufresne, A. Can J Chem 2008, 86, 484.
6. Kamel, S. Expr Polym Lett 2007, 1, 546.
7. Anglès, M. N.; Dufresne, A. Macromolecules 2000, 33, 8344.
8. Anglès, M. N.; Dufresne, A. Macromolecules 2001, 34, 2921.
9. Mathew, A. P.; Thielemans, W.; Dufresne, A. J Appl Polym Sci 2008, 109, 4065.
10. Kvien, I.; Tanem, B. S.; Oksman, K. Biomacromolecules 2005, 6, 3160.
11. Alemdar, A.; Sain, M. Bioresour Technol 2008, 99, 1664.
12. Mathew, A. P.; Dufresne, A. Biomacromolecules 2002, 3, 609.
13. Svagan, A. J.; Hedenqvist, M. S.; Berglund, L. Compos Sci Technol 2009, 69, 500.
14. Chen, Y.; Liu, C.; Chang, P. R.; Cao, X.; Anderson, D. P. Carbohydr Polym 2009, 76, 607.
15. Wan, Y. Z.; Luo, H.; Liang, F. H.; Li, H. X. L. Compos Sci Technol 2009, 69, 1212.
16. Orts, W. J.; Shey, J.; Imam, S. H.; Glenn, G. M.; Guttman, M. E.; Revol, J.–F. J Polym Environ 2005, 13, 301.
17. Teixeira, E. M.; Pasquini, D.; Curvelo, A. A. S. C.; Corradini, E.; Belgacem, M. N.; Dufresne, A. Carbohydr Polym 2009, 78, 422.
18. Teixeira, E. M.; Corrêa, A. C.; Manzoli, A.; Leite, F. L.; Oliveira, C. R.; Mattoso, L. H. C. Cellulose 2010, 3, 595.
19. Buschle-Diller, G.; Zeronian, S. H. J Appl Polym Sci 1992, 45, 967.
20. Hulleman, S. H. D.; Kalisvaart, M. G.; Janssen, F. H. P.; Feil, H.; Vliegenthart, J. F. G. Carbohydr Polym 1999, 39, 351.
21. Sun, Y.; Lin, L.; Pang, C.; Deng, H.; Peng, H.; Li, J.; He, B.; Liu, S. Energy Fuel 2007, 21, 2386.
22. Wang, L.; Kumar, R.; Zhang, L. Front Chem China 2009, 4, 313.
23. Klemm, D.; Heublein, B.; Fink, H. P.; Bohn, A. Angew Chem Int Ed 2005, 44, 3358.